Available online at www.sciencedirect.com
SCIENCE DIRECT
Journal of Molecular Catalysis A: Chemical 251 (2006) 221–228
JOURNAL OF MOLECULAR CATALYSIS A: CHEMICAL
www.elsevier.com/locate/molcata

Understanding the autoxidation of hydrocarbons at the molecular level and consequences for catalysis

Ive Hermans [a,b,*], Pierre A. Jacobs [b], Jozef Peeters [a]

[a] *Division of Quantum Chemistry and Physical Chemistry, Department of Chemistry, KULeuven, Celestijnenlaan 200F, B-3001 Heverlee, Belgium*
[b] *Centre for Surface Chemistry and Catalysis, Department of Microbial and Molecular Systems (M^2S), KULeuven, Kasteelpark Arenberg 23, B-3001 Heverlee, Belgium*

Available online 30 March 2006

Abstract

In this article, we present a thorough study on the autoxidation of cyclohexane, a model substrate for other (saturated) hydrocarbons. Despite the industrial impact of autoxidation reactions, a detailed mechanism is still missing. We present a combined experimental and computational study on the formation of both the major products (cyclohexylhydroperoxide, cyclohexanol and cyclohexanone), and the formation of ring-opened side-products. Up to now, these by-products, mainly adipic acid, were thought to originate from cyclohexanone. However, we found strong evidence that the subsequent propagation of ketone is much slower than assumed, and can only account for some 25% of ring-opened products. On the other hand, the hitherto completely overlooked propagation of the hydroperoxide, via fast αH-abstraction by chain-carrying peroxyl radicals, is identified as the major source of not only alcohol and ketone, but also by-products. In the case of *N*-hydroxyphthalimide (NHPI) catalysed oxidations, where mostly phthalimide *N*-oxyl (PINO•) radicals are propagating the chain, the situation is slightly different, as PINO• reacts more selectively with the alkane substrate than peroxyl radicals. This results in an increase in hydroperoxide selectivity. Lowering of the ROOH concentration by its, e.g. cobalt-catalyzed decomposition, leads to an enhanced catalytic efficiency, as a result of the shift in the $ROO^{\bullet} + NHPI \rightleftharpoons ROOH + PINO^{\bullet}$ equilibrium to the more efficient PINO• chain carrier.

Keywords: Autoxidation; Mechanism; Cyclohexane; Radiacals

1. Introduction

Autoxidation of hydrocarbons such as cyclohexane, *p*-xylene and cumene, is one of the most important large-scale oxy-functionalization processes in the chemical industry [1–4]. It converts raw hydrocarbon material to value-added intermediates such as terephthalic acid and cyclohexanone via a complex set of radical reactions, using molecular oxygen as oxidants. A serious drawback of these reactions is however their radical-chain mechanism, which generally limits the useful reaction yield, as the (primary) products are more reactive than the substrate towards the chain-propagating radical [1–4]. For instance, the autoxidation of cyclohexane is limited to ≤5% conversion where cyclohexylhydroperoxide (CyOOH), cyclohexanone (Q=O, Q stands for $Cy_{-\alpha H}$) and cyclohexanol (CyOH) are the major products [5–7]. A higher conversion results in the appearance of large amounts of ring-opened by-products, mainly adipic acid.

Given the complexity of these reactions, the systematic development of selective catalysts should start with a detailed mechanistic investigation. Although focussing on cyclohexane (CyH) as a model substrate in this paper, conclusions can be extrapolated to other, less demanding substrates.

As is known since long in CyH autoxidation, the homolytic dissociation of CyOOH into $CyO^{\bullet}$ and $^{\bullet}OH$ radicals (reaction (1)) is considered to be the major chain-initiation reaction, while the mutual reaction of two peroxyl radicals (reaction (2)) constitutes the major chain-termination step [1–7].

$$CyOOH \rightarrow CyO^{\bullet} + {}^{\bullet}OH \quad (1)$$

$$CyOO^{\bullet} + CyOO^{\bullet} \rightarrow CyOH + Q{=}O + O_2 \quad (2)$$

The cyclohexylhydroperoxide (CyOOH) is produced in the fast sequence of propagation reactions (3) and (4). At sufficient O_2 pressure, reaction (4) is diffusion controlled and reaction (3)

* Corresponding author. Tel.: +32 16 321648; fax: +32 16 321998.
E-mail address: ive.hermans@chem.kuleuven.be (I. Hermans).

1381-1169/$ – see front matter © 2006 Elsevier B.V. All rights reserved.
doi:10.1016/j.molcata.2006.02.005

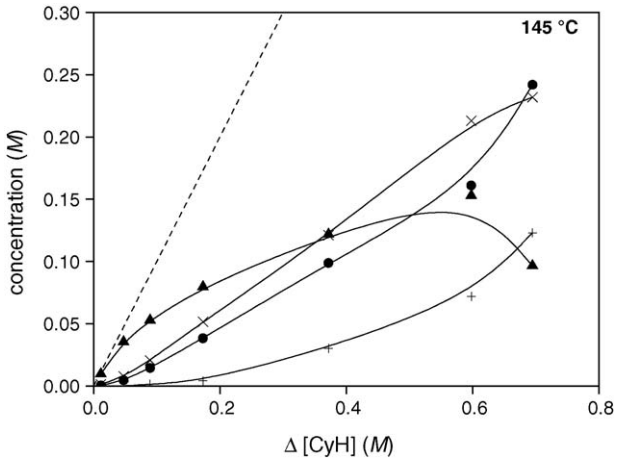

Fig. 1. Product distribution ((▲) CyOOH, (×) CyOH, (●) Q=O, (+) by-products, mainly adipic acid) as a function of the CyH conversion at 145 °C.

is the rate determining step in the overall chain-propagation sequence [1–4].

$$CyOO^{\bullet} + CyH \rightarrow CyOOH + Cy^{\bullet} \quad (3)$$

$$Cy^{\bullet} + O_2 \rightarrow CyOO^{\bullet} \quad (4)$$

It has often been assumed up to now that the ketone is produced exclusively by the termination, (2), while additional alcohol could also originate from the cyclohexoxy radicals (CyO•) by H-abstraction from CyH [1–4]. However, this view is entirely at odds with the large chain-length (=rate of propagation/rate of termination) of ≈100 for the pure autoxidation [1], which dictates unequivocally that the major products must result from propagation steps. Moreover, the evolution of the experimental CyOOH, CyOH and Q=O product concentrations in function of the CyH conversion (see Fig. 1; 145 °C) indicates that the dominating propagation mechanism yields first CyOOH, whereas CyOH and Q=O are formed mainly in subsequent steps.

In a recent publication [8] we identified the fast radical propagation reactions producing CyOH and Q=O. In the present article, we aim (i) to further quantify the propagation steps responsible for the three major products CyOOH, CyOH and Q=O; (ii) to identify the sources of the undesired (carboxyl) by-products; and (iii) to demonstrate the usefulness of this new reaction mechanism in understanding the *N*-hydroxyphthalimide (NHPI)-catalysed oxidation process.

1.1. Theoretical and experimental methods

Potential Energy Surfaces (PES) of the relevant (radical) reactions were characterized using quantum chemical methods that are suitable for the large structures involved, and that were amply validated for the particular types of reaction. At the DFT level we use the Becke three-parameter hybrid exchange functional, combined with the Lee–Yang–Parr non-local correlation functional: B3LYP-DFT [9,10]. Frequency analyses and Intrinsic Reaction Coordinate (IRC) calculations identified the stationary points on the PES as true minima or as Transition States (TSs) connecting reactants and products. However, for some types of reactions, DFT energy-barriers are suspected to be less accurate. Therefore, DFT results are to be compared with higher-level methods, such as G2M [11], G3 [12] or CBS-QB3 [13] results. All calculations were done with the Gaussian 98 software [14]. Cyclohexane (Acros, HPLC) autoxidation was studied experimentally in a stirred (500 rpm) 100 mL stainless steel Parr high-pressure reactor, using 50 mL of cyclohexane and an initial room temperature pressure of 400 psi (=2.76 MPa) pure oxygen. Prior to each experiment, the reactor wall was passivated using a saturated sodium pyrophosphate (Acros, p.a.) solution [15]. The products are analyzed with GC-FID (50 m Cpsil-5, Chrompack column) after silylation with *N*-methyl-*N*-(trimethylsilyl)-trifluoroacetamide (Avocado).

2. Results and discussion

2.1. The pure autoxidation of cyclohexane: radicals caught in the action

2.1.1. Rate of H abstractions

In a previous extensive paper [8], we identified the α-hydrogen (see Scheme 1) abstractions by the chain-carrying peroxyl radicals as crucial subsequent propagation steps in the autoxidation of cyclohexane.

In much of the literature dealing with CyH autoxidation, it is assumed that Q=O is the most important precursor of ring-opened by-products [1–4]. This assumption was inspired by the thermodynamic features of the radical formed after one of the four αH atoms is abstracted: vinoxy resonance is stabilizing this ketonyl radical for about 7 kcal/mol. However, a detailed theoretical analysis of ours [8] reveals that the αH-abstraction by CyOO• radicals is only ≈2–10 times faster than the H-abstraction reaction from the CyH substrate itself. Indeed, at the transition state, the vinoxy stabilisation is only marginally operative and the activation energy is only reduced by 2 kcal/mol with respect to CyH. By monitoring the conversion of initially added (1 mol%) 3-pentanone and cyclopentanone as a function of the CyH conversion, we could measure the reactivity of these two model ketones, relative to CyH, since $\{\Delta[\text{ketone}]/[\text{ketone}]\}/\{\Delta[\text{CyH}]/[\text{CyH}]\} = k(\text{ketone})/k(\text{CyH})$ (for $\Delta[\text{CyH}] \rightarrow 0$) (Fig. 2). The different reactivity – $k(\text{cyclopentanone})/k(\text{CyH}) = 14$ and $k(3\text{-pentanone})/k(\text{CyH}) = 5$ – reflects the difference in the ring strain changes on going from the carbonyl reactants to the TSs. As the calculated barriers (B3LYP/6-311+G(df,pd)/B3LYP/6-31G(d,p)) for the reactions $CH_3OO^{\bullet} + \alpha H$ of 3-pentanone, cyclopentanone and cyclohexanone equal 13.8, 13.5 and 13.95 kcal/mol respectively, this experiment sustains our theoretical prediction of $k(\text{Q=O})/k(\text{CyH}) \approx 2\text{–}10$.

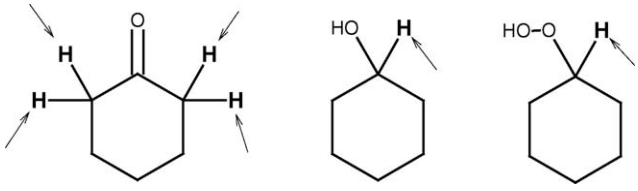

Scheme 1. α-Hydrogen atoms in the reaction products of the CyH autoxidation.

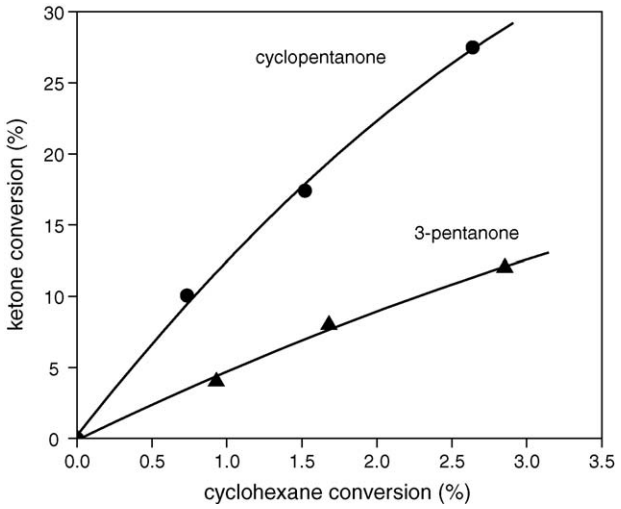

Fig. 2. Comparison between the reactivity of cyclopentanone and 3-pentanone relative to cyclohexane (initially, 1 mol% of ketone was added).

Analogously we determined k(cyclopentanol)/k(CyH) = k(3-pentanol)/k(CyH) = 9 (Fig. 3). As neither of these two substrates contain significant ring strain, both alcohols react equally fast with CyOO$^\bullet$ radicals at the α-position. It can thus be assumed that also k(CyOH)/k(CyH) ≈ 10, again in agreement with our TST predicted value ≈5–20. Exactly the same computational procedure predicts k(CyOOH)/k(CyH) ≈ 20–80 and thus puts forward CyOOH as a promising candidate precursor for the important reaction products.

Below we discuss the reaction of CyOO$^\bullet$ radicals with CyH, CyOOH, CyOH and Q=O separately.

2.1.2. *CyOO$^\bullet$ + CyH*

After the CyOO$^\bullet$ radical has abstracted an H-atom from cyclohexane in the liquid phase, the initial products, CyOOH and Cy$^\bullet$, must diffuse out of the solvent-cage before Cy$^\bullet$ can react with O_2 (reaction (4)). This diffusion process (fraction p),

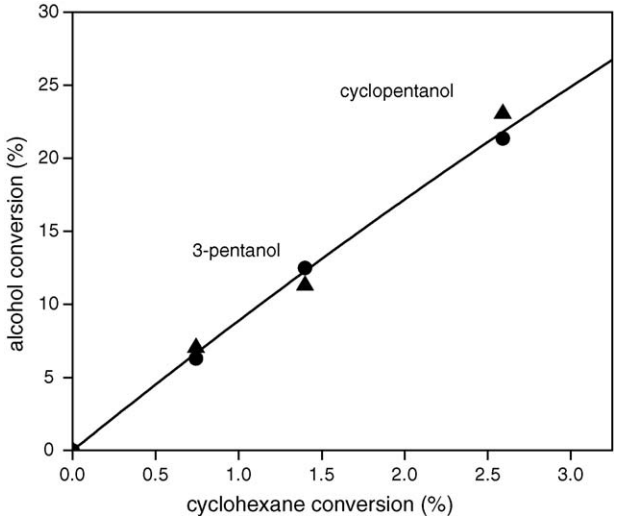

Fig. 3. Comparison between the reactivity of cyclopentanol and 3-pentanol to cyclohexane (initially, 1 mol% of alcohol was added).

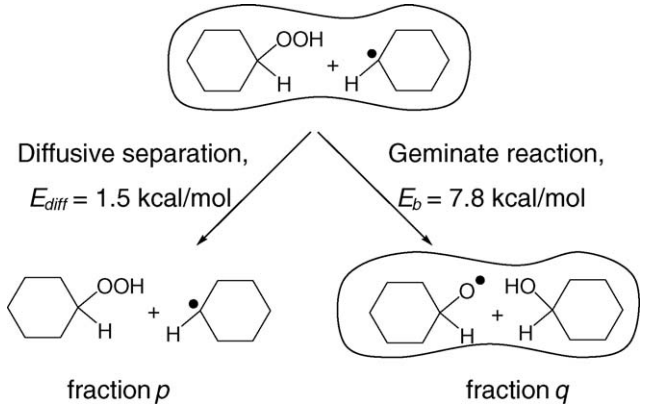

Fig. 4. Competition between diffusive separation of the {CyOOH + Cy$^\bullet$} pair and geminate cage-reaction.

operating at a rate of ≈8×10^9 s^{-1} at 145 °C, stands in competition with a *geminate* cage-reaction between the nascent {CyOOH + Cy$^\bullet$} reactant pair, producing CyO$^\bullet$ + CyOH (fraction q), as shown in Fig. 4. This cage-reaction, although proceeding at a rate of only ≈2.5×10^8 s^{-1} at 145 °C, is thus a competing reaction, producing alcohol directly from the alkane substrate itself. An old experiment, performed by Berezin et al. [5], where ^{14}C-labeled CyOH appeared immediately after ^{14}C-labeled CyH was added to an autoxidation mixture, points to such a direct alcohol channel. It is to be noticed however that the solvent-cage is crucial, as a thermal reaction between free CyOOH and Cy$^\bullet$ radical, as proposed previously [16], can never be competitive with the diffusion-controlled oxygen addition reaction (4). Given that a majority of the CyO$^\bullet$ radicals (≈65%) will react with CyH to produce additional CyOH [17], this reaction explains the experimentally observed [CyOOH]/[CyOH] ratio of 12 at ΔCyH approaching zero.

In the isotope-labeled experiment discussed above, ^{14}C Q=O is only formed after an induction period [5], showing that it is a secondary product formed from primary products (see also Fig. 1).

2.1.3. *CyOO$^\bullet$ + CyOOH*

Next we discuss the fast propagation reaction of the hydroperoxide. Radicals of the type R$_{-\alpha H}$$^\bullet$OOH, as the primary product of CyOO$^\bullet$ + CyOOH, were shown by us to decompose immediately to the corresponding carbonyl compound and $^\bullet$OH, releasing 40 kcal/mol [18]. This is even true for resonance-stabilize examples like C_6H_5-C$^\bullet_{-\alpha H}$HOOH [18]. The $^\bullet$OH radical will rapidly abstract a hydrogen atom from CyH molecules surrounding the {CyOOH + Q=O + $^\bullet$OH} cage, producing even more heat ($\Delta_r H = -22$ kcal/mol) and a Cy$^\bullet$ radical. As such, the CyOO$^\bullet$ + CyOOH + CyH → {CyO$^\bullet$ + Q=O + H_2O + Cy$^\bullet$} reaction produces a nanosized hot-spot of 800–1000 K which can last for about 10–100 ps [8]. Clearly this will affect the fate of the {CyOOH + Q=O + H_2O + Cy$^\bullet$} products, which can either diffuse out of the solvent-cage (fraction r), or can react in a analogous geminate cage-reaction as described above (fraction s), producing CyO$^\bullet$ + Q=O + H_2O + CyOH. As the latter OH-abstraction reaction faces a higher barrier (≈7 kcal/mol) than

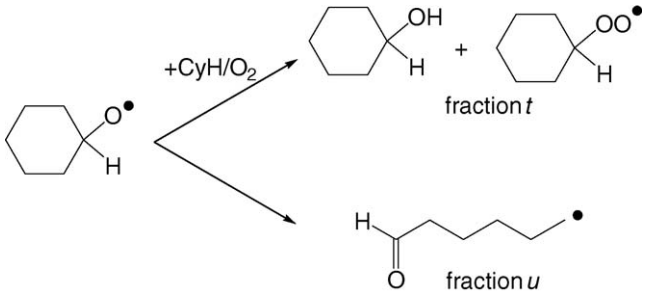

Fig. 5. Reaction paths of the CyO• radicals producing alcohol and ω-formyl radicals.

the diffusion process, the high temperature of the hot-spot will enhance the fraction (s) of caged products that will undergo the geminate cage-reaction. It is thus predicted that CyOOH is the crucial precursor of both Q=O and the bulk of CyOH. As the CyO• radicals produced in the activated cage-reaction can not only react with CyH – producing additional CyOH – but also undergo a β C–C cleavage, yielding the ring-opened ω-formyl radical (CHO–$(CH_2)_4$–CH_2•) [17] as shown in Fig. 5, CyOOH may also be the most important precursor of side products.

2.1.4. CyOO• + CyOH

This αH-abstraction reaction, proceeding at a rate ≈10 times faster than the main propagation reaction CyOO• + CyH, [8] will be followed by a fast O_2 addition, producing the α-hydroxyalkylperoxyl radical Q(OH)OO• (where Q stands for $Cy_{-\alpha H}$). In most of the literature, two important sinks are reported for this radical [2]:

$$Q(OH)OO^{\bullet} + CyH \rightarrow Q(OH)OOH + Cy^{\bullet} \quad (5)$$

$$Q(OH)OO^{\bullet} + CyOO^{\bullet} \rightarrow Q(OH)O^{\bullet} + CyO^{\bullet} + O_2 \quad (6)$$

As was hypothesized [19], there exists another decomposition channel (7):

$$Q(OH)OO \rightleftharpoons Q{=}O + HO_2^{\bullet} \quad (7)$$

An extensive theoretical study of ours [20] revealed that this reaction is much faster ($k(400\,K) = 1.7 \times 10^6\,s^{-1}$) than any other competing process (e.g. H-abstraction from CyH: $k^{\text{first-order}}(400\,K) < 10^3\,s^{-1}$). However, also the reverse rate is large ($k(400\,K) = 1.4 \times 10^{-13}\,cm^3\,s^{-1}$), due to the formation of an H-bonded complex (see Scheme 2) [20]. As such, an equilibrium between the hydroxyperoxyl radicals and the ketone + HO_2• products will be established. This explains why in the pure CyOH autoxidation (small) amounts of Q(OH)OOH are found [19]. As more Q=O is gradually produced, equilibrium (7) shifts to the Q(OH)OO• radicals, and H-abstraction becomes more important, relative to HO_2• formation, in agreement with the experimental data [19].

The importance of mechanism (7) is clear: HO_2• radicals terminate diffusion controlled with other ROO• peroxyl radicals [21] and, as a result, the alcohol co-autoxidation is slowing down the overall RH autoxidation.

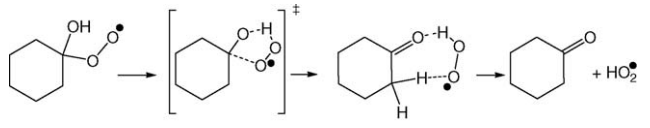

Scheme 2. Unimolecular decomposition of the Q(OH)OO• radicals to Q=O + HO_2•.

2.1.5. CyOO• + Q=O

As we have both experimental and theoretical evidence that the attack of Q=O at one of the four αH atoms is only ≈5 times faster than CyH, the literature view that Q=O is the most important precursor of ring-opened by-products can be seriously questioned. Below, this problem is addressed in more detail.

2.1.6. Detailed stoechiometric and kinetic analysis

Based on the mechanism outlined above, we derived Eq. (8) from a detailed CyOOH balance at low conversions (up to ≈2%):

$$\frac{[CyOH]}{[CyOOH]} \approx \frac{q(1+t)}{p} + \frac{s(1+t')}{p} \times \frac{[Q{=}O]}{[CyOOH]} \quad (8)$$

In this equation, p represents the fraction of {CyOOH + Cy•} which will diffuse out of the solvent cage and form CyOOH + CyOO• and q the fraction which will yield CyO• + CyOH (see Fig. 4); s (=1 − r) is the fraction of {CyOOH + Q=O + H_2O + Cy•} that will form CyO• + Q=O + H_2O + CyOH; t and t' are the fractions of CyO• reacting with CyH/O_2 to form CyOH + CyOO• subsequent to the cage- and activated cage-reactions, respectively, whereas u and u' are the fractions of CyO• decomposing to ω-formyl radicals (see Fig. 5). In Fig. 6 the [CyOH]/[CyOOH] ratio is plotted against the [Q=O]/[CyOOH] ratio; it is seen that Eq. (8) is obeyed for conversions up till 3%, confirming the underlying mechanism. The data thus obtained yield $p \approx 0.95$ and $q \approx 0.05$, in agreement with our model. s is estimated at ≈0.7 ± 0.2 and r at ≈0.3 ± 0.2.

The ratio of slope and intercept, $s(1+t')/q(1+t) = 14 \pm 2$, represents the ratio of CyOH formation from CyOOH over the formation from CyH. The value reflects the difference in temperature of the two cage-reactions producing alcohol (800–1000 K versus 418 K), and the higher barrier for

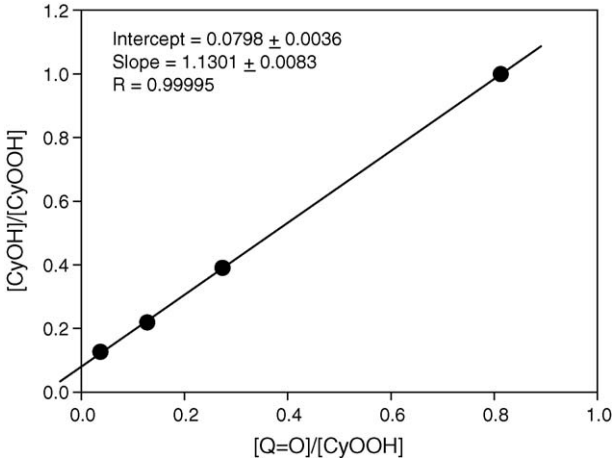

Fig. 6. Plot of the [CyOH]/[CyOOH] ratio vs. [Q=O]/[CyOOH]; validation of Eq. (8), derived from our new reaction mechanism.

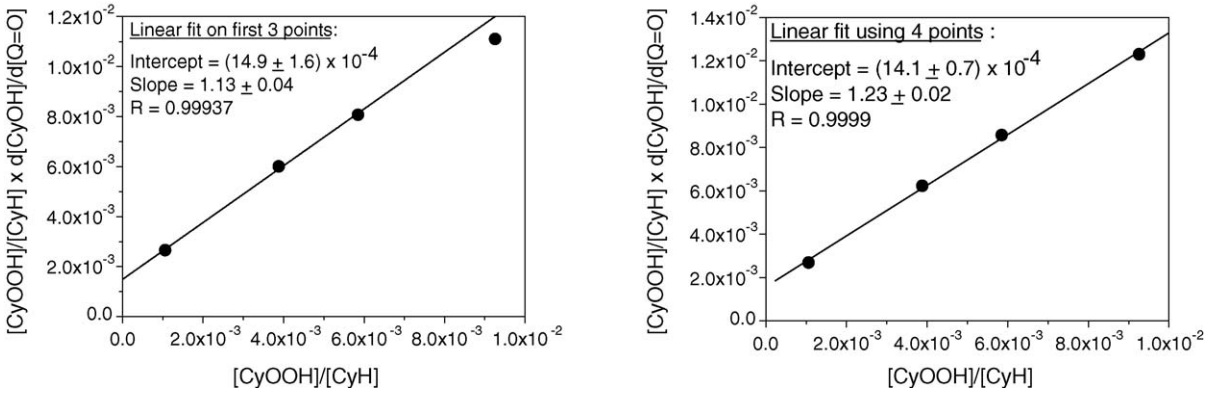

Fig. 7. Plot of the left-hand side (LHS) of Eq. (9) (left) and corrected LHS (right) vs. the [CyOOH]/[CyH] ratio.

the geminate reaction $\{\mathrm{CyOOH} + \mathrm{Cy}^{\bullet}\} \rightarrow \{\mathrm{CyO}^{\bullet} + \mathrm{CyOH}\}$ (≈6.8 kcal/mol) compared to the barrier for diffusive separation (≈1.5 kcal/mol). The expected ratio of branching ratios $(s/r)/(q/p) = \exp[\Delta E/R \times \Delta(1/T)] = 30$ is in keeping with the best experimental estimates $s = 0.7$ and $q = 0.05$, yielding a ratio ≈40.

A detailed analysis of the CyOH and Q=O formation rates leads to Eq. (9)

$$\frac{[\mathrm{CyOOH}]}{[\mathrm{CyH}]} \times \frac{d[\mathrm{CyOH}]}{d[\mathrm{Q{=}O}]} = q(1+t)\frac{k_{\mathrm{CyH}}}{k_{\mathrm{CyOOH}}} + s(1+t')\frac{[\mathrm{CyOOH}]}{[\mathrm{CyH}]} \quad (9)$$

for conversions small enough to ignore the subsequent conversion of CyOH and Q=O ($X \leq 1\%$). In Fig. 7a, the left-hand side (LHS) of Eq. (9) is plotted against the [CyOOH]/[CyH] ratio. The combination of slope and intercept and the $s(1+t')/q(1+t)$ ratio determined above, leads to a $k_{\mathrm{CyOOH}}/k_{\mathrm{CyH}}$ of 54 ± 7, in agreement with our theoretical prediction ≈20–80. As we now know the propagation rates of all important products, relative to CyH, we can correct d[CyOH]/d[Q=O] for the losses due to their subsequent propagation steps, and for formation of Q=O via CyOH co-oxidation. A plot of the so corrected LHS of Eq. (9) is given in Fig. 7b. Slope and intercept do not differ significantly from the uncorrected analysis based on the first three points (Fig. 7a).

This analysis shows unequivocally that both CyOH and Q=O are produced in the fast subsequent propagation steps of CyOOH. This explains the parallel increase of both products as observed in Fig. 1. Below we will investigate the formation of side-products in more detail.

2.1.7. Formation of by-products

One of the most crucial questions to answer is which specie – either Q=O as thought in literature [1–7], or CyOOH as evidenced by our mechanism – is causing the majority of ring-opened by-products. Given the propagation rate of Q=O, relative to CyH, of ≈5, we can easily calculate the relative amount of by-products which can be formed from ketone. As can be seen from Fig. 8, this route can only explain some 20–30% of the observed side-products. To evaluate by-product formation from CyOOH, we have to take into account the fraction of CyOOH consumed that leads to ω-formyl radicals ($=s \times u'$), which than puts the effective side-products formation rate constant at $\approx 20 \pm 10$ relative to the CyH rate constant. For a value of 12, the experimental amount of side products is in perfect agreement with the modelled amount, taking the sum of both the Q=O and CyOOH source (Fig. 8).

An overview of all the important reactions put forward in our new reaction mechanism, is given in Scheme 3.

2.2. Catalysing the propagation: the action of NHPI

The catalytic effect of *N*-hydroxyphthalimide on the oxidation of several hydrocarbons has been the subject of many publications [22–33]. It is generally accepted that phthalimide *N*-oxyl radicals can abstract a hydrogen atom from a hydrocarbon substrate (RH) (see Scheme 4), due to the relatively strong >NO–H bond in NHPI. Subsequently, peroxyl radicals ($\mathrm{ROO}^{\bullet}$) have to abstract an H-atom from NHPI (>NO–H) to regenerate the $\mathrm{PINO}^{\bullet}$ radical. The latter step was first termed as the rate determining step [27], but more recent measurements showed

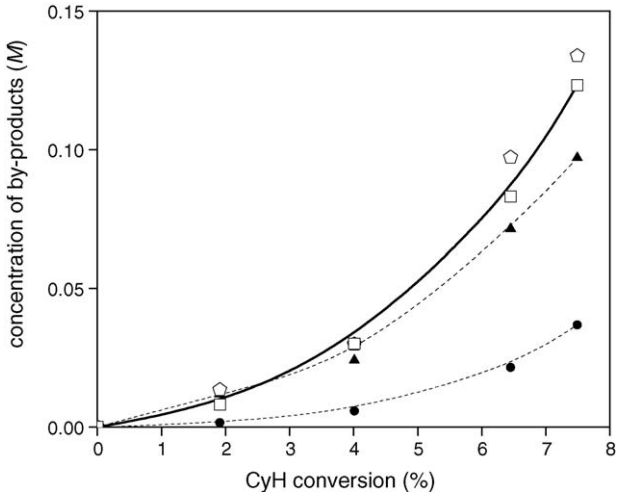

Fig. 8. Comparison between modeled and experimentally determined (□) acid production: (●) represents the contribution of Q=O; (▲) the contribution of CyOOH (adopting an effective side-product formation rate constant of 12, relative to the CyH rate constant); (⬠) is the sum of both contributions.

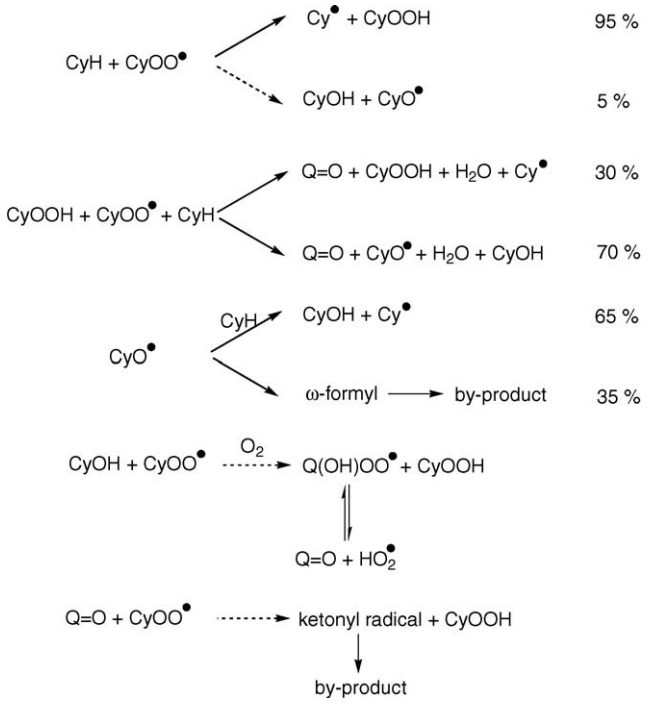

Scheme 3. Important reactions (full arrows) and secondary reactions (broken arrows) during the autoxidation of cyclohexane. Also the estimated branching fractions are given.

that this reaction is very fast [29]. Moreover, our theoretical analysis of this reaction revealed that the ROO• + NHPI reactants should be in equilibrium with the ROOH + PINO• products during autoxidation conditions, as also the reverse reaction is very fast [32]. The catalytic efficiency (C.E.), defined as the ratio of RH oxidation rate in the presence of NHPI over the rate without catalyst, was shown to be given by Eq. (10) [32]:

$$\text{C.E.} = 1 + \frac{k_{\text{PINO}^\bullet}}{k_{\text{ROO}^\bullet}} \times K_{\text{NHPI}} \times \frac{[\text{NHPI}]}{[\text{ROOH}]} \qquad (10)$$

This equation readily explains the observed synergetic effect of $Co(acac)_2$ and $Mn(acac)_2$ [33] on the NHPI catalysed autoxidation: the lowering of [ROOH] by its catalyzed decompostion will shift the equilibrium ROO• + NHPI ⇌ ROOH + PINO• towards the more efficient chain-carrying PINO• radicals. This efficiency of PINO• radicals is not exclusively related to the somewhat large value of k_{PINO} compared to k_{ROO}, but most

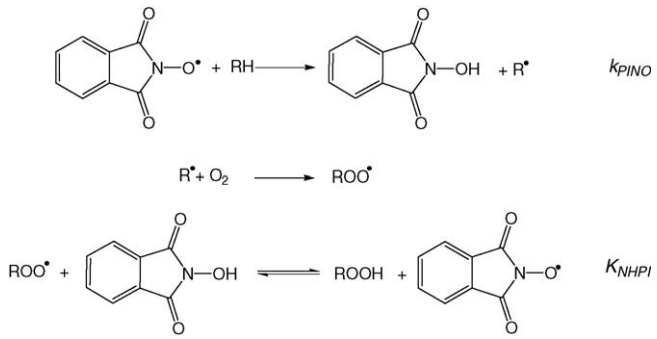

Scheme 4. Reaction of PINO• + RH, and its regeneration via NHPI + ROO•.

Table 1
Barriers (ZPE-corrected) of (α)H-abstraction reactions by >NO• radicals from various substrate molecules at different high levels of theory and at the "DFT" level (values in kcal/mol)

Reaction	G2M//DFT[a]	CBS-QB3	G3	"DFT"[b]
$H_2NO^\bullet + CH_3CH_2CH_3$	25.2	25.5	26.9	25.6
$HN(O^\bullet)CHO + CH_3CH_2CH_3$	17.5	17.3	19.0	18.8
$HN(O^\bullet)CHO + CH_3OOH$	13.4	12.8	14.9	12.7
$HN(O^\bullet)CHO + CH_3OH$	14.2	13.2	15.2	12.8

[a] G2M//DFT represents: E[UCCSD(T)/cc-pVDZ//B3LYP/6-311++G(2df,2pd)] + {E[UMP2/aug-cc-pVTZ//B3LYP/6-311++G(2df,2pd)] − E[UMP2/cc-pVDZ//B3LYP/6-311++G(2df,2pd)]} + ZPE{B3LYP/6-311++G(2df,2pd)}.
[b] "DFT" stands for the B3LYP/6-311++G(df,pd)//B3LYP/6-31G(d,p) level.

importantly to the non-terminating nature of the PINO• radicals [32].

Another conclusion of Eq. (10) is one concerning the design of other, NHPI-like catalysts: one needs a >NO–H compound with a fairly strong O–H bond – as the >NO• radical should be able to readily abstract an H-atom from RH – but not too strong, as this would decrease the equilibrium concentration of the >NO• radicals. For example, at 383 K, it takes 6.6 h to reach 3% CyH conversion (50 mL CyH + 10 mL CH_3CN) when using 1% NHPI, while 1% NHSI (*N*-hydroxysuccinimide) requires 14.2 h. So although the H-abstraction barrier from propane by the >NO• radical from NHSI is ≈2.6 kcal/mol lower (due to a 4.8 kcal/mol stronger >NO–H bond), the C.E. of NHSI is still ≈18 times lower than for NHPI, consistent with the experiment.

An unresolved aspect of NHPI catalyzed reactions is the high concentration of CyOOH (Fig. 9). In order to rationalize this observation, we calculated the rate constant of PINO• + CyOOH, CyOH and Q=O, relative to PINO• + CyH. The B3LYP/6-311++G(df,pd)//B3LYP/6-31G(d,p) level (further referred to as "DFT") was already found to give accurate results for H-abstraction reactions by peroxyl radicals. In Table 1 the same level is now also validated for H-abstractions by >NO• type radicals against the high-level benchmark computational methods G2M [11], G3 [12] and CBS-QB3 [13].

Table 2 summarizes our computational results on the PINO• + CyH/CyOH/CyOOH and Q=O reactions. The effect

Table 2
Thermally averaged energy barriers (ZPE-corrected) for (α-)H-abstraction by PINO• radicals, in kcal mol^{-1} ("DFT" level); and estimated relative rate constants at 400 K

Reaction	Thermally averaged barriers in gas phase[a]	Thermally averaged barriers in CH_3CN[b]	Estimated relative k(400 K)[c]
PINO• + CyH	16.0	19.5	1
PINO• + Q=O	13.5	19.4	0.2–1
PINO• + CyOH	9.0	14.9	2–10
PINO• + CyOOH	8.2	15.9	1–5

[a] At the "DFT" level (B3LYP/6-311++G(df,pd)//B3LYP/6-31G(d,p)).
[b] The solvent effect was evaluated by the Polarized Continuum Model (PCM) [34] at the B3LYP/6-311++G(d,p) level.
[c] Calculated under the assumption that the pre-exponential factor is proportional to the number of H-atoms to be abstracted, and taken into account an entropic factor of 1/5 and 1/3 for the CyOH and CyOOH substrates, respectively, due to the more rigid character of their transition states.

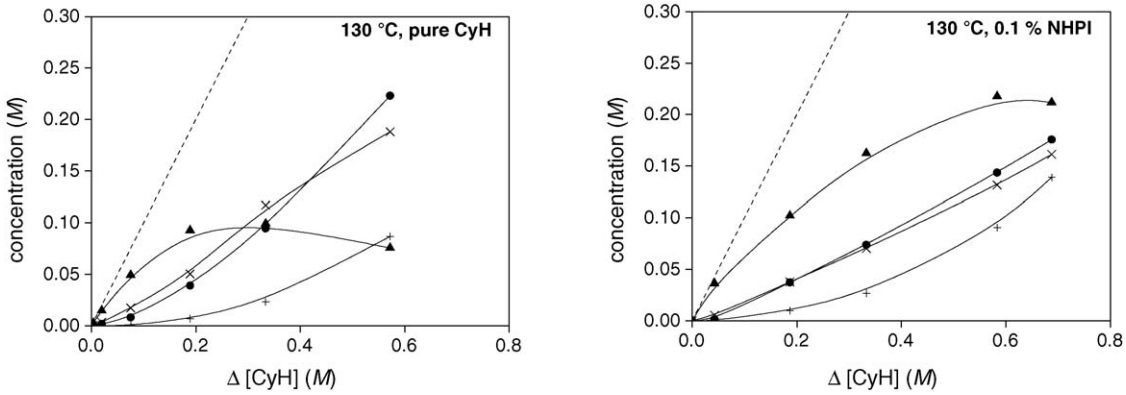

Fig. 9. Product distribution at 130 °C from the autoxidation of 50 mL CyH: left side: pure CyH; right side: +10 mL acetonitrile + 0.1 mol% NHPI. ((▲) CyOOH, (×) CyOH, (●) Q=O, (+) by-products, mainly adipic acid).

of the acetonitrile on the reaction barriers was evaluated by the Polarized Continuum Model (PCM) [34] at the B3LYP/6-311++G(d,p) level, and predicts an increase in activation barrier. This rather large solvent effect is caused by the large decrease in dipole moment when going from the reactants (PINO•: 6.98 Debye) to the TSs (e.g. TS for PINO• + CyH reaction: 3.7 Debye). The relative propagation rates (Table 2) were estimated by assuming that the frequency factor is proportional to the number of abstractable H-atoms. For CyOH and CyOOH, the frequency factor was further reduced by a factor of five and three, respectively, to account for the more rigid character of their TSs (H-bond between reactant and PINO• radical).

These computational results reveal clearly that PINO• radicals react by far more selectively with the CyH substrate than with the (primary) reaction products CyOOH, CyOH and Q=O compared to peroxyl radicals. The difference in the relative rates between PINO• and CyOO• is particularly large for CyOOH. As a result, one can indeed expect a much higher CyOOH selectivity and a lower Q=O and CyOH selectivity. Somewhat surprising is the fairly high concentration of by-products (more or less the same as in the non-catalyzed reaction, see Fig. 9). The reason is that the low reactivity of PINO• towards the αH of CyOOH (relative to CyH), is counteracted by the solvent-enhanced ring-opening of CyO• radicals. Indeed, previous TST calculations showed that this rate can be expressed by the Arrhenius equation $9.8 \times 10^{13}\ \exp(-12.2\,\mathrm{kcal\,mol^{-1}}/RT)\ \mathrm{s^{-1}}$. However, PCM calculations reveal a serious decrease in the decomposition barrier, putting the thermal rate constant at: $k(\mathrm{T}) = 8.95 \times 10^{13}\ \exp(-8.6\,\mathrm{kcal\,mol^{-1}}/RT)\ \mathrm{s^{-1}}$ in CH_3CN. This enhancement of the rate of β-scission of CyO• radicals in polar solvents was also observed experimentally by Ingold and co-workers [35]. This will thus shift the *t*/*u* ratio and explains the rather high concentration of by-products in the NHPI catalyzed reaction.

3. Conclusions

We identified the primary chain-product, CyOOH, as a much more reactive compound than generally assumed so far. It is not only responsible for the chain initiation, but is also the precursor of all other oxygenated compounds. This hitherto unknown role of CyOOH is ascribed to its very fast reaction with chain-carrying peroxyl radicals at its αH-atom. The resulting radical decomposes immediately to Q=O and •OH, which will rapidly abstract a H-atom from the CyH substrate. The overall process $\mathrm{CyOO^\bullet + CyOOH + CyH \rightarrow CyOOH + Q{=}O + H_2O + Cy^\bullet}$ releases more than 60 kcal/mol, causing a local hotspot of 800–1000 K. This high temperature favors the geminate cage-reaction, producing $\mathrm{CyO^\bullet + Q{=}O + H_2O + CyOH}$ over the diffusive separation of $\{\mathrm{CyOOH + Q{=}O + H_2O + Cy^\bullet}\}$. The CyO• radicals thus produced will, partially, decompose to ω-formyl radicals via β-scission and form the most important precursor of by-products.

As this study unequivocally proves that CyOH and Q=O result from fast, subsequent chain-propagation reactions, rather than (slow) termination reactions, the selectivity of autoxidation reactions can be altered by catalyzing the propagation reactions. Indeed, e.g. the PINO• radicals, generated in situ from NHPI, react relatively much more selectively with the CyH substrate than CyOO• peroxyl radicals. As a result, the primary product, CyOOH, is converted more slowly, and its selectivity increases. Due to the established equilibrium, $\mathrm{ROO^\bullet + NHPI \rightleftharpoons ROOH + PINO^\bullet}$, an increased concentration of NHPI must lead to an increased selectivity towards ROOH. The cobalt-catalyzed decomposition of ROOH leads to a synergetic increase in the catalytic efficiency, as it favors the formation of non-terminating PINO• chain-propagators.

It is our further aim to use the qualitative and quantitative data obtained in this study for future design of catalysts.

Acknowledgments

This work is done in the frame of a Belgian IAP-PAI network on catalysis and a GOA on quantum chemistry. I.H. is grateful to the *Fonds voor Wetenschappelijk onderzoek* Vlaanderen for financial support. The authors thank Prof. Dr. Dirk De Vos, Centre for Surface Chemistry and Catalysis for useful discussions.

References

[1] R.A. Sheldon, J.K. Kochi, Metal-Catalyzed Oxidations of Organic compounds, Academic Press, 1981.

[2] C.A. Tolman, J.D. Druliner, M.J. Nappa, N. Herron, in: C.L. Hill (Ed.), Activation and Functionalization of Alkanes, John Wiley & Sons, 1989, p. 303.
[3] G. Franz, R.A. Sheldon, Oxidation, Ullmann's Encyclopedia of Industrial Chemistry, Wiley-VCH, 2000.
[4] S. Bhaduri, D. Mukesh, Homogeneous Catalysis, Mechanisms and Industrial Applications, John Wiley & Sons, 2000.
[5] I.V. Berezin, E.T. Denisov, N.M. Emanuel, The Oxidation of Cyclohexane, Pergamon Press, 1966.
[6] U. Schuchardt, D. Cardoso, R. Sercheli, R. Pereira, R.S. da Cruz, M.C. Guerreiro, D. Mandelli, E.V. Spinacé, E.L. Pires, Appl. Catal. A: Gen. 211 (2001) 1.
[7] M.T. Musser, Cyclohexanol and Cyclohexanone, Ullmann's Encyclopedia of Industrial Chemistry, Wiley-VCH, 2000.
[8] I. Hermans, T.L. Nguyen, P.A. Jacobs, J. Peeters, ChemPhysChem 6 (2005) 637.
[9] A.D. Becke, J. Chem. Phys. 96 (1992) 2115.
[10] C. Lee, W. Yang, R.G. Parr, Phys. Rev. B 37 (1988) 785.
[11] A.M. Mebel, K. Morokuma, M.C. Lin, J. Chem. Phys. 103 (1995) 7414.
[12] L.A. Curtiss, K. Raghavachari, P.C. Redfern, V. Rassolov, J.A. Pople, J. Chem. Phys. 109 (1998) 7764.
[13] J.R. J.A. Montgomery, M.J. Frisch, J.W. Ochterski, G.A. Petersson, J. Chem. Phys. 112 (2000) 6532.
[14] M.J. Frisch, G.W. Trucks, H.B. Schlegel, G.E. Scuseria, M.A. Robb, J.R. Cheeseman, V.G. Zakrzewski, J.A. Montgomery Jr., R.E. Stratmann, J.C. Burant, S. Dapprich, J.M. Millam, A.D. Daniels, K.N. Kudin, M.C. Strain, O. Farkas, J. Tomasi, V. Barone, M. Cossi, R. Cammi, B. Mennucci, C. Pomelli, C. Adamo, S. Clifford, J. Ochterski, G.A. Petersson, P.Y. Ayala, Q. Cui, K. Morokuma, D.K. Malick, A.D. Rabuck, K. Raghavachari, J.B. Foresman, J. Cioslowski, J.V. Ortiz, A.G. Baboul, B.B. Stefanov, G. Liu, A. Liashenko, P. Piskorz, I. Komaromi, R. Gomperts, R.L. Martin, D.J. Fox, T. Keith, M.A. Al-Laham, C.Y. Peng, A. Nanayakkara, C. Gonzalez, M. Challacombe, P.M.W. Gill, B. Johnson, W. Chen, M.W. Wong, J.L. Andres, C. Gonzalez, M. Head-Gordon, E.S. Replogle, J.A. Pople, Gaussian 98, Revision A.7, Gaussian, Inc., Pittsburgh, PA, 1998.
[15] I.L. Arest-Yakubovich, F.A. Geberger, T.V. Khar'kova, L.E. Mitauer, G.Z. Lipkina, Kinet. Katal. 30 (1989) 959.
[16] T.V. Khar'kova, I.L. Arest-Yakubovich, I.L. Lipes, Kinet. Katal. 30 (1998) 954.
[17] J.D. Druliner, P.J. Krusic, G.F. Lehr, C.A. Tolman, J. Org. Chem. 50 (1985) 5838.
[18] L. Vereecken, T.L. Nguyen, I. Hermans, J. Peeters, Chem. Phys. Lett. 393 (2004) 432.
[19] S.V. Puchkov, E.I. Buneeva, A.L. Perkel, Kinet. Catal. 46 (2005) 340.
[20] I. Hermans, J.-F. Müller, T.L. Nguyen, P.A. Jacobs, J. Peeters, J. Phys. Chem. A 109 (2005) 4303.
[21] D.M. Rowley, R. Lesclaux, P.D. Lightfoot, B. Nozière, T.J. Wallington, M.D. Hurley, J. Phys. Chem. 96 (1992) 4889.
[22] Y. Yoshino, Y. Hayashi, T. Iwahama, S. Sakaguchi, Y. Ishii, J. Org. Chem. 62 (1997) 6810.
[23] B.B. Wentzel, M.P.J. Donners, P.L. Alsters, M.C. Feiters, R.J.M. Nolte, Tetrahedron 56 (2000) 7797.
[24] R. Arnaud, A. Milet, C. Adamo, C. Einhorn, J. Einhorn, J. Chem. Soc., Perkin Trans 2 (2002) 1967.
[25] Y. Ishii, S. Sakaguchi, T. Iwahama, Adv. Synth. Catal. 343 (2001) 393.
[26] F. Minisci, C. Punta, F. Recupero, F. Fontana, G.F. Pedulli, J. Org. Chem. 67 (2002) 2671.
[27] R. Amorati, M. Lucarini, V. Mugnaini, G.F. Pedulli, J. Org. Chem. 68 (2003) 1747.
[28] B. Saha, N. Koshino, J.H. Espenson, J. Phys. Chem. A 108 (2004) 425.
[29] F. Minisci, F. Recupero, A. Cecchetto, C. Gambarotti, C. Punta, R. Faletti, R. Paganelli, G.F. Pedulli, Eur. J. Org. Chem. (2004) 109.
[30] Y. Cai, N. Koshino, B. Saha, J.H. Espenson, J. Org. Chem. 70 (2005) 238.
[31] R.A. Sheldon, I.W.C.E. Arends, Adv. Synth. Catal. 346 (2004) 1051.
[32] I. Hermans, L. Vereecken, P.A. Jacobs, J. Peeters, Chem. Commum. (2004) 1140.
[33] Y. Ishii, S. Sakaguchi, Catal. Surv. Jpn. 3 (1999) 27.
[34] E.G.S. Miertus, E. Scrocco, J. Tomasi, Chem. Phys. 55 (1981) 117.
[35] D.V. Avila, C.E. Brown, K.U. Ingold, J. Lusztyk, J. Am. Chem. Soc. 115 (1993) 2929.